

Enhancement of Efficiency in Large area Multicrystalline Silicon Solar Cells by Metallization and Texturization

S K RATH¹, R M PUJAHARI^{2,+}, C K DAS¹ and M C ADHIKARY¹

¹Dept. of Applied Physics and Ballistics, F M University, Balasore, India

²ABESIT, Ghaziabad, India

⁺Corresponding author, E-mail: rpujahari@gmail.com

Received: 27.11.2017 ; Revised : 12.12.2017 ; Accepted :8.1.2018

Abstract. Isotropic single step acid texturing using a combination of HF-HNO₃-CH₃COOH acids at a controlled temperature is easy, low cost and convenient option for photovoltaic industry. Grain boundary smoothening throughout the large area multicrystalline silicon (mc-Si) solar cell surface by texturization process optimization enhances cell efficiency. In the fabrication of Solar cell, metallization is an important step responsible for proper ohmic contact of the crystalline silicon cells with an efficiency more than 15%. In our present study atomic force microscope is used to observe their intragrain surface in a miniscule area of 3 μ m \times 3 μ m. This AFM study of surface roughness gives a comprehensive idea of surface by the three dimensional analysis. So stainless steel (SS316) screen printing is the most suitable process for its low cost, flexibility and high productivity. In our case the exact height and width of the silver (Ag) grid fingers of both 2D screen printed cells and 3D screen printed cells are measured by an innovative Telestep equipment. In this paper the result shows a reduction of shadowing loss of 0.7% for 3DSP cells which is a welcome result for the fabrication of large area mc-Si solar cell fabrication. Again series resistance and shadowing loss minimisation result into higher efficiency of 16% in case of 3DSP cells keeping other fabrication steps the same.

Keywords. Multicrystalline silicon solar cell; HF-HNO₃-CH₃COOH texturization, AFM study, roughness and section analysis, 3D screen printing; Telestep stylus measurement;

1. Introduction

Surface control of multicrystalline silicon (mC-Si) solar cells by texturing is one of the critical issues of high efficiency large area low cost industrial cells in mass production level. The direction dependent anisotropic alkaline texturization

solution is standard for monocrystalline silicon solar cells [1]. This anisotropic etching often results in high surface roughness due to different etch rates of the solution for different crystal orientations in mC-Si solar cells. There are other alternate texturization processes available for mC-Si with their own advantages and disadvantages. The very common acidic etchant using hydrofluoric (HF), nitric (HNO_3) and acetic (CH_3COOH) acids give isotropic fast etching of silicon surface [2]. After this texturing silicon surface becomes smoother irrespective of grain orientations and hence surface reflectivity enhances. However, the excessive controls required for etching solution during etching process and the cost of chemicals restrict its use over specific purposes only. An isotropic etching process containing HF- HNO_3 -de-ionized (DI) water etching step followed by HF- HNO_3 etching step provides one good texturization option [3, 4]. It has two main advantages. Firstly, it forms rounded surface having better antireflection property in place of flat silicon surface formed by acid texturing using HF- HNO_3 -DI water combination. Secondly, it helps to form shallow front junction to enhance cell blue response [5] by the reduction of dead layer [6]. However, the control parameters again involved in this process require costly equipments, costly chemicals and hence this process may be suitable only to photovoltaic plants of very large capacity. Hence, people often opt for only direction dependent silicon etching by high concentration sodium hydroxide (NaOH) or potassium hydroxide (KOH) solution [7] as a cheaper and convenient option, although, this process leads to severe leakage loss in voltage because of different grain orientations in the wafer. A recently developed low cost chemical texturing for industrial mC-Si solar cell involving NaOH-NaOCl (sodium hypochlorite) offers an easy and low cost production alternative [8, 9]. This optimized etching solution does not have any effect on mC-Si grain boundaries [10-12] and thus has an excellent isotropic etch characteristics to enhance parameters like V_{oc} and fill factor (FF). Additionally, the evolution of chlorine during silicon etching process removes the additional chlorine neutralization step which is generally must for process involving NaOH [8].

Screen printing technique provides a cost-effective alternative to the complicated metallisation processes due to which it has already been a widely accepted method in solar cell industries [2]. However, for metallization of the emitter surface the most important task is to control the series resistance loss after cell fabrication. The main problem encountered in screen printing metallization is poor contact quality that results in poor fill factor of the fabricated cells. Metal contact with silicon surface depends on several parameters such as surface

condition, emitter surface concentration and dopant impurity profile [3], anti-reflection coating (ARC) on the emitter surface, screen parameters, metal pastes and above all, the firing profile. Optimization of front and back contacts for the solar cell is the ultimate task for process designers. Therefore the requirement is not only to reduce the effects of series resistance (R_s) by enhancing the cell fill factor (FF), but also to increase the short circuit current (I_{sc}) by the reduction of the shadowing loss without compromising with production output.

2. Experimental

A. Cell fabrication

Boron doped p-type $0.5 - 3 \Omega\text{-cm}$ resistivity Deutsche Solar mC-Si wafers of 5 inch square are taken for the present study. For the acid polishing process, the acid solution comprising HF ($\approx 49\%$), HNO_3 ($\approx 69\%$), CH_3COOH mixed in a 3:5:3 ratio (by volume) is prepared. The etching bath is made of stainless steel (SS316) and bath temperature is maintained at $7-8^\circ\text{C}$ with the help of external cooling jacket. DI water from a constant temperature bath (maintained at 7°C) is circulated through the cooling jackets. 20 wafers are loaded in a Teflon jig and they are polished in the acid solution for 30 seconds. Nitrogen gas is bubbled inside the polishing solution so that it acts as a stirrer during the polishing process. Immediately after polishing the wafers are rinsed in DI water for nearly 15 minute till no acidic smell is coming out from the wafers. The acid polishing is an exothermic process, so immediately after polishing the temperature of the bath is increased and the solution becomes brownish. For polishing of the next batch of 20 wafers, the solution is again cooled down to 7°C and then only the next batch texturization is performed. In the fresh texturization solution we are able to polish 12 batches i.e., 240 wafers are polished at a time. Representative wafer as sample is then analyzed using Atomic Force Microscopy (AFM)

B. Metallization

For the front emitter metallization, two batches of 40 wafers each, are taken after back aluminium and silver-aluminium printing. First 40 wafers are then screen printed on the front surfaces by 2D 325 and the other 40 wafers by 3D SS 325 screens [13, 14]. After printing and cofiring, one cell from each batch is taken as the representative for the 2D and 3D screen printing processes.

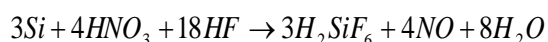
C. Characterization

Small pieces of dimension $2 \text{ cm} \times 2 \text{ cm}$ are cut from the representative cells of 2D and 3D screen printing categories by using Nd-YAG laser for the surface

reflectance analysis by spectrophotometer[15]. Before the surface analysis, wafer pieces (as samples) are cleaned ultrasonically in isopropyl alcohol followed by rinsing in DI water and drying. These samples containing only the grid lines are taken from the same areas of both the cells. The DIV and LIV characteristics of the cells are also measured. Their LIV characteristics are measured under 1 SUN intensity with AM1.5 Global spectrum [16].

3. Results and discussion

The main objectives and purpose of texturization is in increasing the efficiency of the silicon solar cell. This can be considerably done by reducing the reflection losses and a creating a damage-free Si-surface prior to diffusion. In the acid polishing process, the chemical reaction is given below [2].



This redox reaction points on the silicon surface randomly become oxidation or reduction sites and they act like localized electrochemical cells. Each point becomes both an anode and cathode site over time. For uniform etching the time spent on each point should be the same. The oxidizing agent HNO_3 oxidizes silicon surface isotropically and the complexing agent HF dissolves the SiO_2 layer with itself by forming an H_2SiF_6 complex. HNO_2 is regenerated by this autocatalytic reaction. The oxidizing power of the etchant is set by the amount of unassociated HNO_3 . The diluting CH_3COOH controls the speed of the reaction to some extent. It has low dielectric constant as compared to DI water. This assists in less dissociation of HNO_3 and yields higher oxidation power for the etchant. Also less polar nature of CH_3COOH provides proper wetting of slightly hydrophobic silicon surface. With the formation of H_2SiF_6 complex exposed layers of silicon are etched away from the mC-Si wafer. The rate of reaction is quite fast and strongly exothermic [1]; hence maintaining the solution at a low temperature is a mandatory requirement for this polishing process. The main objective 3D screen printing metallization is to increase the efficiency of the multicrystalline silicon solar cell.

The total value R_s is calculated by linking the individual resistances i.e., resistance of metal semiconductor on entire back surface (R1), resistance of semiconductor material base (R2), resistance in the emitter between two grid fingers (R3), metal-semiconductor contact resistance under the grid finger (R4), resistance of the grid finger (R5) and resistance of the bus bar (R6). The values of R1 and R2 are neglected for practical cases for being too small [9]. In our case of

metallization, the contact material and finger width are correctly selected, therefore R4 also makes no significant contribution. Also for the 2DSP and 3DSP cells busbar resistance (R6) has been assumed to have the same value. So practically for analysis of Rs, the contributions of R3 and R5 have to be determined.

The value of R3 between the grid fingers is given as [9]

$$R_3 = \frac{\rho_{\square} d}{l} \quad (1)$$

Here ρ_{\square} is sheet resistivity of the Ag grid finger, 'd' is the spacing between the fingers and 'l' is the length of the finger. R_3 is calculated separately for cells of both types using eqn. (1). Fig.1 indicates telestep profiles of two consecutive Ag-grid fingers for a 3DSP cell in a single scan. We have $l = 118$ mm from our grid design data and $\rho_{\square} = 5\text{m}\Omega/\text{sqr}$ [10]. Also from Fig.3 for the 2DSP cell, we have $d = 2.37\text{mm}$ to have the value of R_3 as $0.167\text{m}\Omega$. So for the 3DSP cell value of R_3 is calculated as $0.1659\text{m}\Omega$ taking $d = 2.35\text{mm}$, l and ρ_{\square} values remain the same as used for the case of 2DSP cell. Comparing the obtained values of R_3 i.e. $0.167\text{m}\Omega$ (for the 2DSP cell) and $0.1659\text{m}\Omega$ (for the 3DSP cell) it has been concluded that there is a marginal decrease in the value of R_3 ($< 1\%$) in case of the 3DSP cell.

Again the R5 is given by [9]

$$R_5 = \frac{1}{3} \rho_{\text{met}} \frac{l}{aL} \quad (2)$$

Here ρ_{met} is the resistivity of metal [10], 'a' is the thickness of the finger and 'L' is the width of the finger. All the experimentally determined screen printed parameters from Fig.4 are listed in Table-I. Using $\rho_{\text{met}} = 4.8 \times 10^{-10} \Omega\text{-m}$ [11], in eqn (2) the value of R_5 is calculated as $7.99\text{m}\Omega$. For the 3DSP cell, with the experimental value from Table-I the value of R_5 is calculated as $7.01\text{m}\Omega$ with ρ_{met} remaining same. Theoretical value of Rs is calculated by adding R_3 and R_5 and the values for Rs are $8.1\text{m}\Omega$ and $7.1\text{m}\Omega$ for the 2DSP and 3DSP cell respectively which are very close to the experimental values. This indicates that the experimental data for the height and width of finger ascertains that the series resistance values of the 3DSP cells is 10-13% lower as compared to the 2DSP cells.

Table 1. 2DSP and 3DSP Screen Printed Parameters as Measured by Stylus.

| Screen used | D(mm) | a(μm) | L(μm) | R3(m Ω) | R5(m Ω) | Rs(m Ω) |
|-------------|-------|--------------------|--------------------|-----------------|-----------------|-----------------|
| 2D | 2.35 | 12.45 | 196 | 0.1674 | 7.99 | 8.1 |
| 3D | 2.37 | 15.03 | 0.1659 | 7.01 | 7.1 | |

Again the difference in L values for 2DSP and 3DSP cell as given in Table. I is 17 μm . Ag metal coverage for the 3DSP cell and the 2DSP cell from the emitter surface are 121mm X 179 μm and 121mm X 196 μm respectively. This shows a percentage reduction in shadowing loss of 0.7% in case of 3DSP cell compared to the 2DSP cell.

A major impact of excellent emitter metallization is clearly visible in the significant improvement in FF of the 3DSP cell as compared to the 2DSP one. This upgradation of the I_{sc} and FF results into an improvement of cell efficiency from 14.7% (2DSP) to 16% (3DSP) without any major variation in cell fabrication techniques.

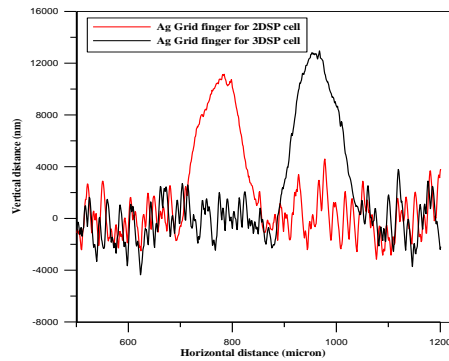


Figure 1. Telestep Profiles of Ag-grid Fingers of 2DSP and 3DSP cells

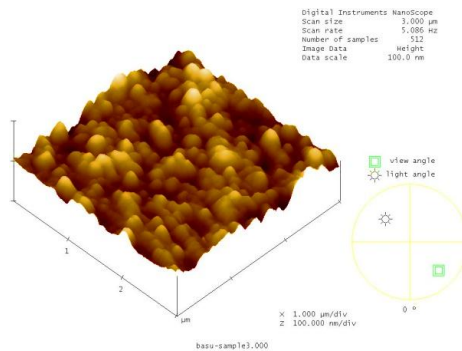


Figure 2. Three dimensional surface of Acid textured mC-Si wafer as observed by AFM

The AFM studies are performed on these wafers over an area of $3\ \mu\text{m} \times 3\ \mu\text{m}$. Fig.2 represents a three dimensional AFM micrograph for our textured wafer showing Excellent smoothness. The slow and controlled polishing leads to polished peaks of low height as observed from the AFM image in Fig.2.

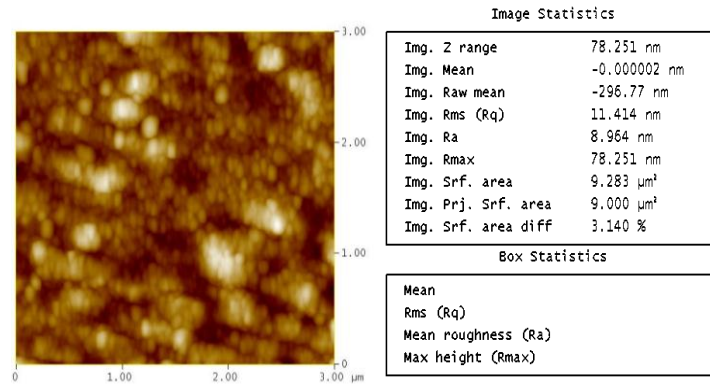


Figure 3. Two dimensional surface of Acid textured mC-Si wafer as observed by AFM

From the 2D analysis and roughness mapping (shown in Fig.3), it is observed that during the alkali polishing the surface becomes more regular with bumps of wide base and have uniform flatter top surface. Also area of each individual white mark (indicating surface of height more than 75nm) is more in Fig.3. Intragrain roughness study by AFM indicates that the standard deviation of the heights within the scanned region gives the quantitative value of the quality of roughness of the polished surface (represented by the parameter ‘ R_q ’) is measured 11.414 nm only.

The details statistical data of the surface mapping is given in Fig.4. It shows that standard deviation of the values of height between the reference markers (rms) is 4.933 nm in the acid polishing solution. Difference between the highest and lowest points (R_{max}) on the sectional profile relative to the center line over the length of the roughness curve (L) is 11.054 nm for the acid polished sample for $L = 117.19\text{nm}$ and radius of the peak height (R) is 158.32 nm. All these values clearly indicates about excellent flat surface for our textured silicon sample, which is responsible for better electrical performance of the devices made using it.

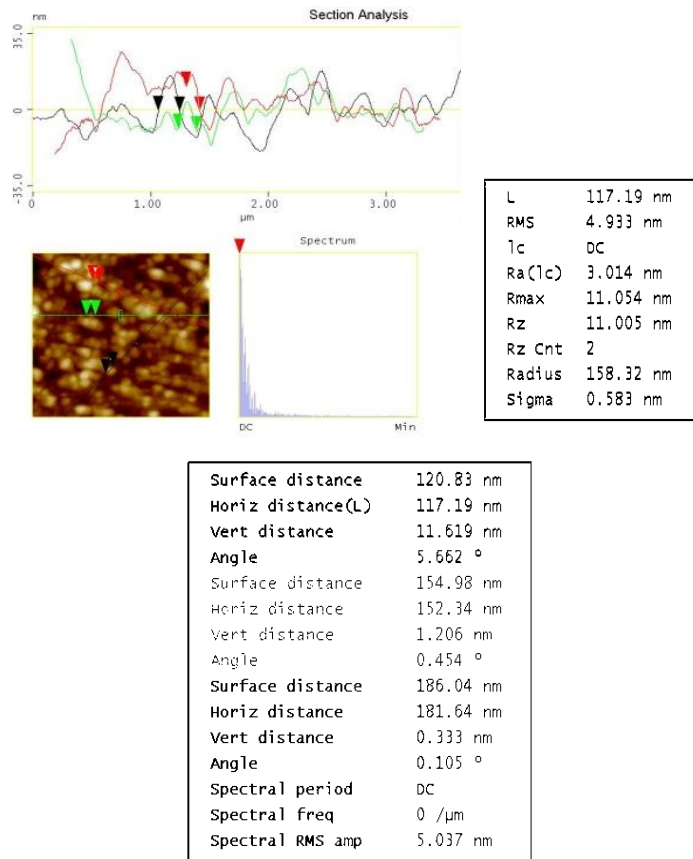


Figure 4. Section analysis and mapping of Acid textured mC-Si wafer as observed by AFM

4. Conclusion

The nanometric surface roughness study by AFM for the acid wet texturization or polishing processes for industrial mC-Si solar cells is performed. Our study clearly indicates the excellent surface smoothness of HF-HNO₃-CH₃COOH textured mC-Si industrial solar wafers and also ascertains better efficiency industrial solar cells coupled with a proper anti-reflecting coating over it.

The increase in metal heights during the 3DSP of the emitter surface layer is quite large. Higher height of front silver decreases both the shadowing loss and metal resistance. It resulted into a marginal decrease of reflectivity by 0.13% in 300 nm to 1200 nm wavelength range. The value of Rs obtained after calculating R3 and R5 as 8.1 mΩ and 7.1 mΩ for 2DSP and 3DSP cells respectively which

are quite close to the experimental values 8.2m Ω and 7.3m Ω . Low series resistance value (7.1m Ω) of the 3DSP cell enhances cell FF upto 0.764, which is also responsible for the increase in the cell efficiency. In a cumulative effect the cell efficiency enhances from 14.7% to 15.5% without any other change in the regular production line. Also higher height eases soldering with solder plated copper strip and creates strong bonding between them at tabbing step during module fabrication.

Acknowledgements

The authors express their sincere thanks to P.G. Dept. of Applied Physics and Ballistics, FM University, Balasore, India and ABESIT, Ghaziabad for continuous stimulation and support for the present research.

References

- [1] A. Ebony, Y. H. Cho, M. Hilalii, A. Rohatgi and D. Ruby; *Solar Energy Materials and Solar Cells*, (2002), **74**, p.51.
- [2] M Bohm, E Urbanski, A E Delahoy and Z Kiss, *Solar Cells*, **20**, 155(1987).
- [3] PK Basu, BC Chakravarty, SN Singh, P Dutta and R Kesavan, *Solar Energy Materials and Solar Cells*, **43**, 15 (1996)
- [4] U Gangopadhyay, SK Dhungel, PK Basu, SK Dutta, H Saha and Junsin Yi, *Solar Energy Materials and Solar Cells*, **91**, 285(2007)
- [5] PK Basu, H Dhasmana, D Varandani, BR Mehta and DK Thakur, *Solar Energy Materials and Solar Cells*, **93**, 1743 (2009)
- [6] PK Basu, H Dhasmana, N Udayakumar and DK Thakur, *Renewable Energy*, **34**, 2571 (2009)
- [7] E Vazsonyi, Z Vertesy, A Toth and J Szlufcik, *Journal of Micromechanics and Microengineering*, **13**, 165 (2003)
- [8] U Gangopadhyay, SK Dhungel, PK Basu, SK Dutta, H Saha and Junsin Yi, *Solar Energy Materials and Solar Cells*, **91**, 285 (2007)
- [9] MC Adhikary, RM Pujahari, *Journal of Energy and Power Resources*.ISSN:Print-2333-9136,Online-2333-9144(2014)
- [10] PK Basu, RM Pujahari, H Kaur, D Singh, D. Varandani and BR Mehta, *Solar Energy, Elsevier*, **84**, 1658 (2010)
- [11] R M Pujahari , M C Adhikary, *ISST Journal of Applied Physics*.ISSN:0976-903X, **Vol-5** No.1(2014)

- [12] D Singh, RM Pujahari, H Kaur and PK Basu *ISST Journal of Applied Physics*.ISSN:0976-903X, **1**(2), 9 (2010)
- [13] RM Pujahari, MC Adhikary, 12th *International Congress on Renewable Energy (ICORE-2014)*, ISBN: 978-81-8454-150-2, Manekshaw Centre, New Delhi, Organised by Solar Energy Society of India, December 8-9, p.251-254, 2014.
- [14] M C Adhikary, RM Pujahari, *International Congress on Renewable Energy (ICORE-2013)*, ISBN: 978-93-82880-80-6, KIIT University, Bhubaneswar, Organised by *Solar Energy Society of India*, November 27-29, p.181-186, 2013.
- [15] RM Pujahari, D Singh, and PK Basu, *International Conference on Applications of Renewable Energy Utilization (ICREU-2012)*, Coimbatore Institute of Technology, Coimbatore, Tamil Nadu, India, Jointly with Oklahoma State University, Stillwater, USA, January 4-6,p-4-5 , 2012.
- [16] RM Pujahari, D Singh, and PK Basu, *International Conference on Applications of Renewable & Sustainable Energy(REIS-2010)*,Department of Physics, Under UGC SAP Programme, Osmania University, Hyderabad, December 16-18, , 2010.
- [17] RM Pujahari, H Kaur, D Singh, and P K Basu, *International Conference on Renewable Energy (ICARE-2010)*, ISBN : 13978-81-909984-0-6, Maulana Azad National Institute of Technology, Bhopal, June 26-28, Vol.1, p-157-162, 2010.